A GENERIC HARMONIC ROTOR MODEL FOR HELICOPTER FLIGHT SIMULATION

M. Chaimovich, A. Rosen and O. Rand
Faculty of Aerospace Engineering
Technion - Israel Institute of Technology
Haifa 32000, Israel

Abstract

A new rotor model for helicopters flight mechanics simulation is presented. The rotor dynamics is described using multiblade coordinates. the aerodynamic loads include nonlinear effects such as stall and compressibility. These loads are described as harmonic series. The number of harmonics in the series determines the model accuracy. Thus by changing the number of harmonics from one to a large number, it is possible to obtain models that range between a Tip Path. Plane approach and an accurate blade-element model. The user of the model can very easily change the model accuracy and consequently it efficiency. The new rotor model is investigated and its application for trim and maneuver calculations is presented and discussed.

1. Introduction

The main rotor is the most important component of any helicopter. Because of its importance and relative complexity, the main rotor is usually the most sophisticated and time consuming element in any code for flight simulation of helicopters. There are several approaches currently used for modeling the main rotor for helicopter simulations. These include 1) the direct blade-element approach, 2) the "closed form" Tip-Path-Plane (TPP) approach and 3) the rotor-map approach.

The direct blade-element approach includes a straightforward integration of the equations of motion of the blade. This approach enables to take into account any distribution of properties (mass and aerodynamic) along the blade. In addition, it allows the use of very sophisticated nonlinear aerodynamic models. Because of the complexity involved, a numerical approach is needed. One of the first blade-element models was presented by Gessow and Crim (Refs. 1,2). Since then various direct blade-element models were presented. Descriptions and references to various models can be found in almost any text-book on helicopters (see Refs. 3-5). An example of a more recent application of the direct blade-element method for helicopter simulation is presented in Ref. 6.

While the direct blade-element method is probably the accurate one among the above mentioned approaches, it requires a large computing effort because of the detailed azimuthal integration of the blade's equations of motion. The blade's dynamics has a much smaller typical time constant compared to the helicopter fuselage dynamics. Thus the integration of the rotor dynamics accounts for most of the computing effort.

Codes for flight mechanics simulations always represent well thought compromises between simplicity (namely efficiency) and accuracy. Therefore, in order to increase the model efficiency, the above mentioned two other approaches to rotor modeling have been widely used.

The closed-form TPP approach represents the "opposite" of the direct blade-element approach. In this approach the blade equations of motion are integrated analytically after adopting the TPP description of the rotor motion. Closed form expression for the TPP variables and the loads, which are transferred from the rotor to the helicopter fuselage, are obtained. These variables are obtained as functions of the fuselage motion and pilot/AFCS commands. It is clear that by using such a model the calculations which are associated with the rotor are drastically reduced. TPP rotor models were used quite extensively during the years and the interested reader may find more details on these models in Refs. 3-6. More recent examples of TPP rotor models for flight mechanics purposes, are described in Refs. 7,8.

While TPP models are very efficient, they present a major drawback. Since a closed form analytic integration of the blade equations of motion is required, only relatively simple aerodynamic models can be used. These aerodynamic models are usually linear and do not include nonlinear effects such as stall or compressibility. These limitations restrict the use of the TPP models since they may result in increasing errors at important regions of the helicopter flight envelope, such as flying at high airspeeds or operation at high rotor loads.

The third kind of approach to rotor modeling, namely the rotor-map, is aimed at over coming the aerodynamic weakness of the TPP approach, while retaining similar efficiency. In this approach, a nonreal-time blade-element model is run off-line for a great number of flight conditions and the results are recorded in quasi-static look-up tables. The tables are then used by the real time rotor module to instantly determine the quasi-static rotor forces, moments and attitudes based on the input parameters. Rotor dynamics are then added to the quasi-static results to complete the rotor output. Although it offers a better aerodynamic representation, this approach is still restrictive with regard to modeling

dynamic and aerodynamic secondary effects. An example of a rotor-map approach is the rotor model in FLYRT (Ref. 9).

The purpose of this paper is to present a new generic harmonic rotor model for helicopter flight simulation. The model is based on a harmonic representation of all the aerodynamic loads that act on the blades. The number of harmonics which are used in the rotor model determine its accuracy. Increasing the number of harmonics increases the accuracy, but at the same time also increases the computing effort which is associated with the main rotor calculations. The new rotor model presents a high level of flexibility. If one chooses to use only the first harmonic then he obtains a model which is dynamically equivalent to the TPP model, but where nonlinear aerodynamic effects (such as compressibility and stall) are taken into account. On the other hand, by taking a very high number of harmonics the model becomes equivalent to a direct blade-element model. The transformation from one level of the model to another is very convenient. Practically it is achieved by changing only a single parameter in the input to the computer code, the parameter that determines the number of harmonics in the main rotor model.

The paper will start with a detailed description of the new rotor model. The equations of motion of single blade will be derived using Lagrange method. Then the equations of motion of the entire rotor will be obtained by applying a multiblade coordinate transformation. Afterwards the method of calculating the harmonics of the aerodynamic loads will be explained.

The new rotor model will be combined with an existing model for a helicopter flight simulation. Then parametric studies of the rotor model itself and its use for helicopter trim and maneuver calculations, will be presented and discussed.

2. The Rotor Equations of Motion

2.1 A single blade kinematics

The present single blade kinematics is similar to the kinematics that was presented in Refs. 10, 11. Because there are some differences in notation, and for the sake of completeness, this kinematic will be described briefly again.

As shown in Fig. 1, each blade is attached to the hub at an offset e. The azimuth angle of the representative blade is ψ, measured counterclock wise from the backward direction (negative X_{FH} direction. X_{FH}, Y_{FH}, Z_{FH} are the hub nonrotating system of coordinates). The blade motion includes a rigid body flapping angle β, a root pitch angle θ_R and a cross sectional elastic pitch θ_F. X_B, Y_B, Z_B are the coordinates of the blade "material" system. X_B lies along the blade axis, while Y_B and Z_B are the cross section coordinates. These coordinates are attached to the blade and rotate with it due to flapping or root and elastic pitch variations. X_B becomes zero at the blade root and is equal to L (the blade length) at the tip. A linear approximation is used to describe the elastic pitch variations, thus:

$$\theta_F = \theta_e X_B/L \qquad (1)$$

β, θ_R and θ_e of each blade are the unknowns that define the blade dynamics. The model also allows for a flap/pitch coupling, thus flapping is associated with a pitch variation ($K_1\beta$) at the root. Lead-lag motions are neglected since usually their influence on flight mechanics problems of articulated rotors is very small.

2.2 The equations of motion of a single blade

The equations of motion are derived by using the Lagrange method. For that purpose the complete expressions for the kinetic energy and potential energy of the blade are derived. The contributions to the potential energy include a linear flapping spring and a pitch spring at the root, accompanied by elastic pitch variations along the blade. The potential energy becomes:

$$U_k = \frac{1}{2} K_\beta \beta^2 + \frac{1}{2} K_\theta (\theta_R - \theta_p)^2 + \frac{1}{2} K_{TB} \theta_e^2 \qquad (2)$$

K_β and K_θ are the linear flexibilities of the flapping and root pitch springs. K_{TB} represents the equivalent elastic flexibility of the blade. θ_p is the pitch command at the blade root as given by the pilot or the helicopter Automatic Flight Control System (AFCS).

The blade system includes also damping and thus Rayleigh's dissipation function is also included in the system's Lagrangian. This dissipation function, D_B, is given by:

$$D_B = \frac{1}{2} C_{RT} (\dot{\theta}_R - \dot{\theta}_p)^2 + \frac{1}{2} C_{TB} \dot{\theta}_e^2 \qquad (3)$$

C_{RT} is the pitch control system damping while C_{TB} is the structural damping of the elastic pitch variations along the blade.

Since the complete expression for the kinetic energy is quite complicated, a symbolic manipulation code is used in order to derive the equations. The complete equations of motion are fairly complicated

and include many small terms. Thus an ordering scheme is adopted in order to simplify the equations. This ordering scheme is based on the fact that the angles β, θ_R and θ_e are small. In addition, it is also assumed that the helicopter pitch, roll and yaw rates are small compared to the rotor angular velocity (Ω), and the helicopter linear accelerations are small compared to typical centripetal accelerations at the blade tip. The three coupled equations of motion of the blade become:

$$[A]\{\ddot{\sigma}_b\} + \Omega[B]\{\dot{\sigma}_b\} + \Omega^2[C]\{\sigma_b\} + [W']\{S\} +$$

$$a_z\{a_z\} + \{a\} + \{pc\} = \{Q_i\} \qquad (4)$$

$\{\sigma_b\}$ is the blade vector of unknowns defined as:

$$\{\sigma_b\}^T = <\beta,\theta_R,\theta_e> \qquad (5)$$

$\{S\}$ is the vector of the blade angular rates and accelerations, defined as:

$$\{S\}^T=<q\sin\psi - p\cos\psi,\ q\cos\psi + p\sin\psi,$$

$$\dot{q}\sin\psi - \dot{p}\cos\psi,\ \dot{q}\cos\psi + \dot{p}\sin\psi> \qquad (6)$$

where p and q are the roll and pitch rates, respectively, of the rotor hub about the X_{HF} and Y_{HF} axes) a_z in Eq. (4) is the normal acceleration (in the direction of the shaft of the rotor, while $\{pc\}$ is the pitch-command vector, defined as:

$$\{pc\}^T = <0,\ -K_\theta\theta_p - C_{RT}\dot{\theta}_p,\ 0> \qquad (7)$$

The coefficients' matrices [A], [B], [C], [W'], and the vectors $\{a_z\}$, $\{a\}$, are defined in Ref. 20.

$\{Q_i\}$ in Eq. (4) is the vector of generalized forces, defined as:

$$\{Q_i\}^T = <Q_{\beta A} + Q_{\beta G},\ Q_{\theta RA} + Q_{\theta RG},\ \theta_{\theta eA} + \theta_{\theta eG}> \qquad (8)$$

The indices β, θ_R and θe define the generalized coordinate to which the generalized force refer (β, θ_R and θ_e, respectively), while the subscripts A and G indicate aerodynamic or gravity contributions.

The expressions for the generalized forces are obtained by applying the principle of virtual work.

The components of the aerodynamic force per unit length of the blade are denoted: f_{ABX}, f_{ABY}, f_{ABZ}, in the directions X_B, Y_B and Z_B, respectively. In addition there is an aerodynamic moment about the blade aerodynamic center, m_{ABX}, per unit length. After applying the principle of virtual-work and using the ordering scheme, the following expressions for the generalized aerodynamic forces are obtained:

$$Q_{\beta A} = \int_0^L (f_{ABZ}X_B + m_{ABX}K1)dX_B \qquad (9a)$$

$$Q_{\theta RA} = -\int_0^L (f_{ABZ}Y_{ac} - m_{ABX})dX_B \qquad (9b)$$

$$Q_{\theta eA} = -\int_0^L (f_{ABZ}Y_{ac} - m_{ABX})X_B dX_B/L \qquad (9c)$$

Y_{ac} and Z_{ac} are the cross sectional coordinates of the aerodynamic center. Since Z_{ac} is usually very small its influence is neglected.

The generalized gravity forces are:

$$Q_{\beta G} = g_s \cdot I1 \qquad (10a)$$

$$Q_{\theta RG} = Q_{\theta eG} = 0 \qquad (10b)$$

g_s is the component of the gravity acceleration in the shaft direction. Equations (10a,b) are obtained after assuming that cross sectional center of mass coordinates Y_{cg} and Z_{cg}, are small.

2.3 The multiblade coordinate transformation

In the previous subsection the equations of motion of a single blade were derived. In order to obtain the equations of motion of the rotor as a whole, it is convenient to use a Multiblade Coordinate Transformation (MCT). The MCT details depend on the number of blades. In what follows derivations for a four bladed rotor will be presented. The same procedure can be followed for any other number of blades.

Consider for example the flapping angles (β^m is the flapping angle of the mth blade). The multiblade coordinates are defined as follows:

$$\beta_0 = \frac{1}{4}\sum_{m=1}^{4}\beta^m \qquad (11a)$$

$$\beta_{1c} = \frac{1}{2}\sum_{m=1}^{4}\beta^m\cos\psi_m \qquad (11b)$$

$$\beta_{1s} = \frac{1}{2} \sum_{m=1}^{4} \beta^m \cos\psi_m \qquad (11c)$$

$$\beta_{N/2} = \frac{1}{4} \sum_{m=1}^{4} \beta^m (-1)^m \qquad (11d)$$

$$\psi_m = \psi + (m-1) \cdot \pi/2 \qquad (11e)$$

Similar expressions exist for the other variables, θ_R^m and θ_e^m.

As will be shown, it is very convenient to express the generalized aerodynamic forces in a series form, as follows:

$$Q_{\beta A} = M_{\beta 0} + \sum_{j=1}^{N_j} [M_{\beta C_j} \cos(j\psi) + M_{\beta S_j} \sin(j\psi)] \qquad (12a)$$

$$Q_{\theta RA} = M_{\theta R0} + \sum_{j=1}^{N_j} [M_{\theta RC_j} \cos(j\psi) + M_{\theta RS_j} \sin(j\psi)] \qquad (12b)$$

$$Q_{\theta eA} = M_{\theta e0} + \sum_{j=1}^{N_j} [M_{\theta eC_j} \cos(j\psi) + M_{\theta eS_j} \sin(j\psi)] \qquad (12c)$$

N_j is the number of harmonics which are included in the expressions of the generalized aerodynamic forces. As mentioned above and as will be shown in what follows, this parameter has a very significant influence on the efficiency and accuracy of the results of the rotor model. In addition a standard pitch control is assumed:

$$\theta_p = \theta_{0p} - A_{1p}\cos\psi - B_{1p}\sin\psi \qquad (13a)$$

$$\dot{\theta}_p = \dot{\theta}_{0p} - [\dot{A}_{1p} + B_{1p}\Omega]\cos\psi - [\dot{B}_{1p} - A_{1p}\Omega]\sin\psi \qquad (13b)$$

Using the regular technique of transforming the single blade equations of motion (Eq. (4)), into the equations of motion of the entire rotor (MCT), the following system of twelve coupled equations is obtained (three equations for each of the four blades):

$$[A_A]\{\ddot{\sigma}\} + [B_B]\{\dot{\sigma}\} + [C_C]\{\sigma\} + [PC']\{PC\} +$$

$$[PC]\{PC\} + a_z\{a_1\} + \{a_2\} + [W'_{W'}]\{pq\} = \{M_A\} \qquad (14)$$

$\{\sigma\}$ is the vector of rotor dynamic unknowns:

$$\{\sigma\}^T = \langle \beta_0, \theta_{R0}, \theta_{e0}, \beta_{1C}, \theta_{1RC}, \theta_{1eC}, \beta_{1S}, \theta_{1RS}, \theta_{1eS},$$

$$\beta_{N/2}, \theta_{RN/2}, \theta_{eN/2} \rangle \qquad (15)$$

$\{PC\}$ is the pilot command vector:

$$\{PC\}^T = \langle \theta_{0p}, A_{1p}, B_{1p} \rangle \qquad (16)$$

$\{pq\}$ is the vector of angular rates and angular accelerations:

$$\{pq\}^T = \langle q, p, \dot{q}, \dot{p} \rangle \qquad (17)$$

The matrices $[A_A]$, $[B_B]$, $[C_C]$, $[PC']$, $[PC]$, $[W'_{W'}]$ and vectors $\{a_1\}$ and $\{a_2\}$ are defined in Ref. (20).

$\{M_A\}$ is the vector of generalized loads that includes mainly aerodynamic contributions. This twelve order vector is assembled of four vectors of order three, as follows:

$$\{M_A\}^T = \langle \{Q_{A0}\}^T, \{Q_{AC}\}^T, \{Q_{AS}\}^T, \{Q_{AN/2}\}^T \rangle \qquad (18)$$

The vectors $\{Q_{A0}\}$ are defined below:

$$\{Q_{A0}\}^T = \langle M_{\beta 0} + Q_{\beta G} + \sum_{j=4,8\ldots}^{N_j} M_{\beta C_j} \cos(j\psi) +$$

$$\sum_{j=4,8\ldots}^{N_j} M_{\beta S_j} \sin(j\psi),\ M_{\theta R0} + \sum_{j=4,8\ldots}^{N_j} M_{\theta RC_j} \cos(j\psi) +$$

$$\sum_{j=4,8\ldots}^{N_j} M_{\theta RS_j} \sin(j\psi),\ M_{\theta e0} + \sum_{j=4,8\ldots}^{N_j} M_{\theta eC_j} \cos(j\psi) +$$

$$\sum_{j=4,8\ldots}^{N_j} M_{\theta eS_j} \sin(j\psi) \rangle \qquad (19)$$

Similar expressions for the other terms in Eq. (18) may be found in Ref. 20. Equation (19) indicatesthat the number of harmonics which are included in the expressions that describe the generalized aerodynamic loads, Eqs. (12a-c), have a direct influence on the vector $\{M_A\}$. But this influence, as in the case of

helicopter vibrations, is filtered in a special manner while adding the contributions of all the blades. Thus only certain discrete harmonics have an influence on each element of the vector $\{M_A\}$.

3. Calculating the Generalized Aerodynamic Forces

3.1 The cross sectional aerodynamic loads

Every calculation of the cross sectional aerodynamic loads starts with a computation of the cross sectional incoming flow velocity components, U_p and U_T (see Fig. 1). These components include the

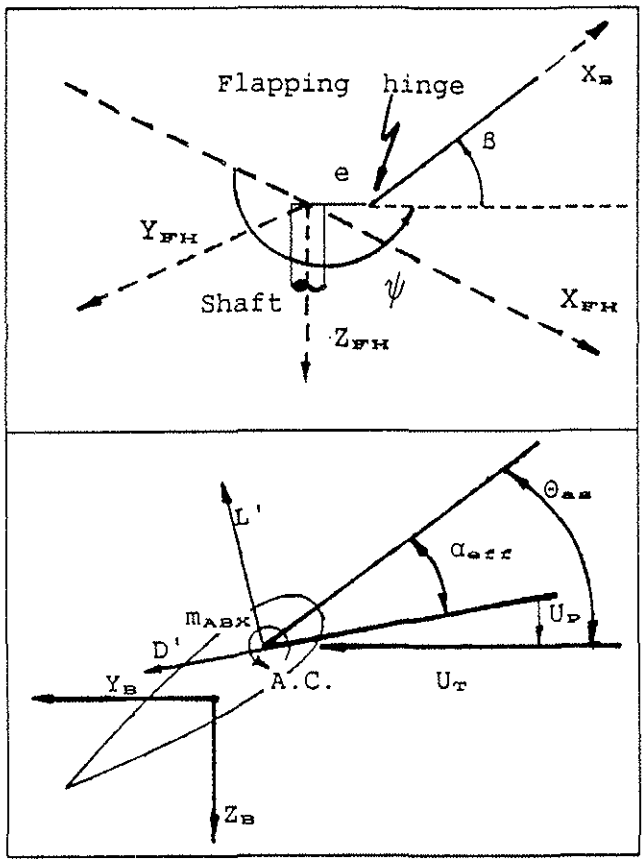

Fig. 1. Geometric description and notation.

contributions of the fuselage motion, the rotor rotation, and the blade motion relative to the hub. In addition, the influence of the induced velocity is also included. Only the normal component of the induced velocity is taken into account and it includes two main parts: the "steady" part and a dynamic inflow component which is a result of dynamic variations of the rotor aerodynamic loads.

The general expression for the "steady" inflow is given below:

$$\lambda_i = (v_i/\Omega R) = \lambda_{io} f_{\lambda io}(X) + \lambda_{ic} f_{\lambda ic}(X)\cos\psi_w + \lambda_{is} f_{\lambda is}(X)\sin\psi_w \quad (20a)$$

where:

$$X = (e+X_B)/R \quad (20b)$$

v_i is the dimensional normal component of the induced velocity. $f_{\lambda io}(X)$, $f_{\lambda ic}(X)$ and $f_{\lambda is}(X)$ are general functions of the radial coordinate X. ψ_w is the azimuth angle relative to hub-wind coordinates, where:

$$\psi_w = \psi + \beta_w \quad (21)$$

β_w is the rotor side-slip angle.

In the present model Glauert's uniform inflow (Ref. 12) or a linear longitudinal inflow distributions according to White and Blake (Ref. 13) are used.

The dynamic inflow model is based on the model of Pitt & Peters (Ref. 14). The dynamic variations of the inflow are described by the following expressions:

$$\Delta\lambda_i = \Delta\lambda_{io} + \Delta\lambda_{ic} X\cos\psi_w + \Delta\lambda_{is} X\cos\psi_w \quad (22)$$

$\Delta\lambda_{io}$, $\Delta\lambda_{ic}$ and $\Delta\lambda_{is}$ represent variations of the induced velocity due to dynamic variations of the rotor thrust and aerodynamic pitch and roll moments (relative to a certain trimmed flight condition).

Based on two dimensional considerations, the cross sectional lift, drag and moment per unit length, L', D' and M'_{A1}, respectively, are calculated.

In addition to the aerodynamic moment as given by the two dimensional "quasi-steady" approach, a damping moment is also added according to the two dimensional unsteady aerodynamic model of Theodorsen (see Ref. 15):

$$M'_{A2} = -\pi\rho\tilde{U}C^3(\dot{\theta}_R + X_B\dot{\theta}_e/L + K1\dot{\beta})/8 \quad (23)$$

The resultant cross sectional aerodynamic force components and aerodynamic moment, per unit length (see Eqs. (9a-c)), are determined by the components of the above loads in the X_B, Y_B, Z_B directions.

3.2 Calculating the generalized aerodynamic forces

A substitution of the above cross sectional aerodynamic loads into Eqs. (9a-c), results in the generalized aerodynamic forces as functions of the azimuth angle ψ. The integration along the blade is performed by applying the Gauss method of order eight, which has been found to be accurate and

efficient compared to other methods.

As indicated by Eqs. (12a-c), the generalized aerodynamic forces, which are periodic functions of ψ, are expressed in a series form. In order to calculate the coefficients of these series, all the generalized forces are calculated at different azimuthal locations, and then the coefficients are obtained by using well known formulations of Fourier series. Thus the coefficient in Eq. (12a) are obtained after using the following equations:

$$M_{\beta 0} = \frac{1}{2\pi}\int_0^{2\pi} Q_{\beta A}(\psi)d\psi \qquad (24a)$$

$$M_{\beta C_j} = \frac{1}{\pi}\int_0^{2\pi} Q_{\beta A}(\psi)\cos(j\psi)d\psi \qquad (24b)$$

$$M_{\beta S_j} = \frac{1}{\pi}\int_0^{2\pi} Q_{\beta A}(\psi)\sin(j\psi)d\psi \qquad (24c)$$

The coefficients of the other two generalized aerodynamic forces are calculated in a similar manner.

In addition to applying Eqs. (24a-c), use can also be made of the FFT method in order to calculate the harmonic coefficients. In what follows an investigation of the required number of azimuthal points, and a comparison between using Eqs. (24a-c) and an FFT method, will be presented.

4. The Helicopter Flight Simulation

4.1 Calculating the rotor loads

A crucial step in any helicopter flight simulation is the calculation of the loads which are exerted on the fuselage by the rotor. By also expressing the rotating blade loads as series in the azimuthal angle ψ, similar to the series of the generalized loads that were described above, it becomes relatively convenient to add up the contributions of all the blades, in order to obtain the resultant rotor loads.

Special care is necessary while transferring the loads from the rotating blade system to the hub nonrotating system of coordinates, X_{FH}, Y_{FH} and Z_{FH} (see Fig. 1).

Since the high frequency components of the loads are not important in flight mechanics problems, they are neglected. The rotor loads acting on the fuselage (at the hub center point) are the force $\overline{F}_R$ and the moment $\overline{M}_R$, as described by their components in the $\hat{X}_{FH}$, $\hat{Y}_{FH}$ and $\hat{Z}_{FH}$ directions (these are unit vectors in the coordinates directions X_{FH}, Y_{FH} and Z_{FH}, respectively):

$$\overline{F}_R = H_R\hat{X}_{FH} + Y_{FH}\hat{Y}_{FH} - T_R\hat{Z}_{FH} \qquad (25)$$

$$\overline{M}_R = L_R\hat{X}_{FH} + M_R\hat{Y}_{FH} + Q_R\hat{Z}_{FH} \qquad (26)$$

All the components in Eqs. (25,26) are closed form known functions of the rotor variables and blade's loads are described above. It is worth mentioning again that these components depend on the number of harmonics which are retained in all the rotor calculations.

4.2 The complete helicopter model

The equations of motion of the rotor (that were described above) are combined with the equations of motion of the helicopter fuselage. The two sets of equations are highly coupled since the force and moment which are exerted by the main rotor on the fuselage are crucial factors in determining the fuselage response, while the rotor dynamics is largely influenced by the fuselage motions. The technique which is used in order to solve the coupled equations was used previously by Beigelman and Rosen (Ref. 8). According to this technique the rotor and fuselage equations of motion are integrated separately. Since the rotor dynamics is much faster than the fuselage dynamics, separate integrations lead to different time steps in both integrations (much longer typical time steps in the integration of the fuselage equations of motion) and thus the required computer effort is reduced. A special updating procedure is used in order to transfer the necessary information between the fuselage and rotor models. This updating includes the rotor loads that act on the fuselage, and on the other hand the hub motion which is an important input to the rotor equations of motion.

The fuselage equations of motion include the contributions of the fuselage aerodynamics, the various horizontal and vertical aerodynamic surfaces (vertical fin, longitudinal stabilizer, wings), tail rotor and external stores. The way in which these components are treated is similar to the modeling technique that was presented in Ref. 16, and improved later on for maneuver simulations in Ref. 8.

4.3 The solution of the equations of motion

Trimmed flight is a special case where all the fuselage linear velocity components and angular rates are constant (as indicated above, vibrations at high frequencies are ignored). In this case the fuselage

equations of motion, which are nonlinear coupled ordinary differential equations in the general case, become a system of nonlinear algebraic equations. On the other hand, all the rotor variables are in general periodic functions of the azimuth angle of the rotor. Thus the rotor equations of motion are solved by using the method of Ref. 17. the coupled rotor/fuselage equations are simultaneously solved by applying a nonlinear numerical solver.

Every simulation of maneuvers starts from a certain trimmed flight condition. The pilot commands are fed into the model and the equations of motion are integrated with time. As indicated above, the rotor and fuselage equations of motion are integrated separately, using a special continuous updating procedure between the two models.

5. Results and Discussion

In what follows the new rotor model and its use are investigated. The investigation starts with an isolated rotor where the influence of different parameters on the results and convergence properties are studied. Afterwards trim calculations and maneuvers simulations are presented and discussed. All the examples that are presented deal with the AH-64 (Apache) helicopter and its rotor. The investigation concentrates on the special aspects of the present model which are the convergence with respect to the number of harmonics and the calculations of the harmonic coefficients.

5.1 Calculations of an isolated rotor

As explained above, the aerodynamic loads are expressed as series and only a finite number of harmonics, N_j, are retained in the calculations. Thus in the case of every aerodynamic load it is possible to consider two forms of this load: There is the "actual" load which is calculated by using the derivations of section 3 and the complete blade motions. On the other hand there is the "approximate" load which is used throughout the rotor calculations, which include only N_j harmonics of the infinite series which is necessary in order to describe the "actual" load. As N_j is increased, it is clear that the difference between the "actual" and "approximate" aerodynamic loads is decreasing. Thus this difference can be used as a measure of the convergence of the model.

In Fig. 2a the resultant lift force of a single blade, as a function of the blade azimuth angle, is presented at an airspeed of 130 knots. Four cases of retaining between one to four harmonics, in the expressions of the aerodynamic loads, are presented. In each case the "actual" and "approximate" loads are compared. While in the case of one harmonic there are relatively large differences between the two, these differences decrease very rapidly as N_j increases. In the case of four harmonics only very small differences exist. It is expected that the influence of higher harmonics increases with the airspeed. Figure 2b is similar to Fig. 2a, except that the airspeed is reduced to 80 knots. In both cases the rotor is practically producing the same thrust. It can be seen that, as expected, the convergence in this case is much faster. Three harmonics give almost a perfect convergence, while even one harmonic shows much smaller differences between the "actual" and "approximate" lift, as compared to the situation at 130 knots.

Similar results are also obtained when other variables, like the resultant drag force or the aerodynamic flapping moment, are considered.

The reason for the need for higher harmonics at increasing airspeeds, is shown very clearly in Figs. 3a,b. In these figures the spanwise distributions of the Mach number and angle of attack, at four azimuth angles (ψ=0°, 90°, 180°, 270°), at airspeeds of 130 knots (Fig. 3a) and 80 knots (Fig. 3b), are presented. The increases in the magnitude of the azimuthal variations at 130 knots, compared to 80 knots, are clearly seen. These azimuthal variations result in an increase in the number of harmonics that are necessary for convergence.

In Figs. 2a,b the convergence was investigated by comparing the "actual" and "approximate" aerodynamic loads. It is also interesting to check the convergence by comparing the "actual" aerodynamic loads as the number of harmonics is increased. In Fig. 4 the variation of the actual lift force, as N_j is increased, is shown. The convergence as N_j increases is seen very clearly, but it should be noted that there are some differences between the curves for N_j=3 and N_j=4, although these differences are much smaller than the differences between N_j=2 and N_j=3. In the figure the one-per-rev. components, in all the cases, are also plotted. It is interesting to note that inspite of the existing differences between the "actual" loads, the one-per-rev components practically coincide. Since the one-per-rev component is the most important one, this indicates that for various purposes good results may be obtained by using even one harmonic.

As expected, similar investigation for 80 knots shows much better harmonic convergence and the one-per-rev components of all the cases practically coincide.

As explained in subsection 3.2, the harmonic coefficients of the aerodynamic loads are obtained after calculating the aerodynamic loads at several azimuthal locations. The values of the aerodynamic loads at these azimuthal locations are substituted

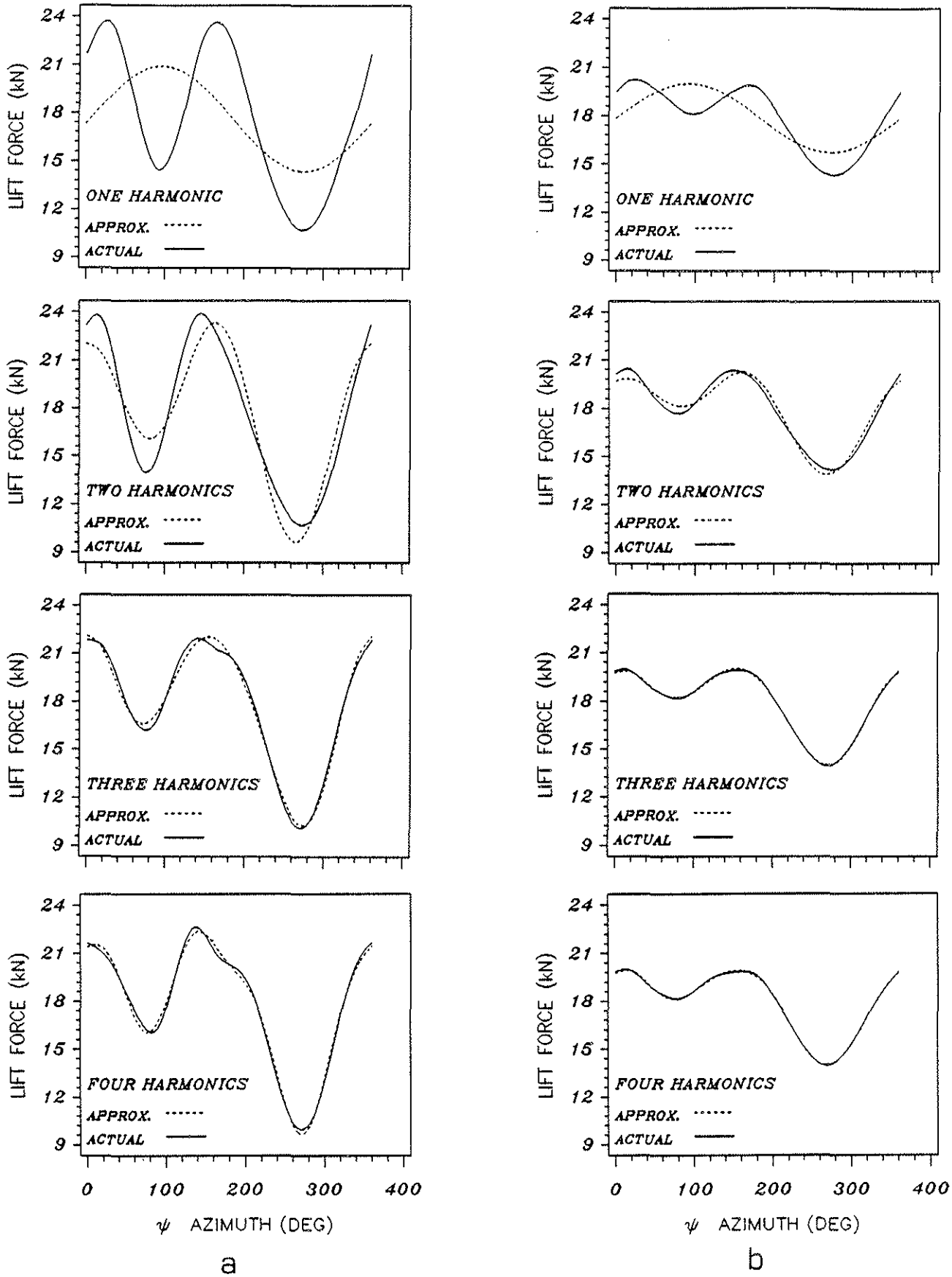

Fig. 2. The influence of the number of harmonics on the difference between the "actual" and "approximate" resultant lift force of a blade. a) 130 knots, b) 80 knots.

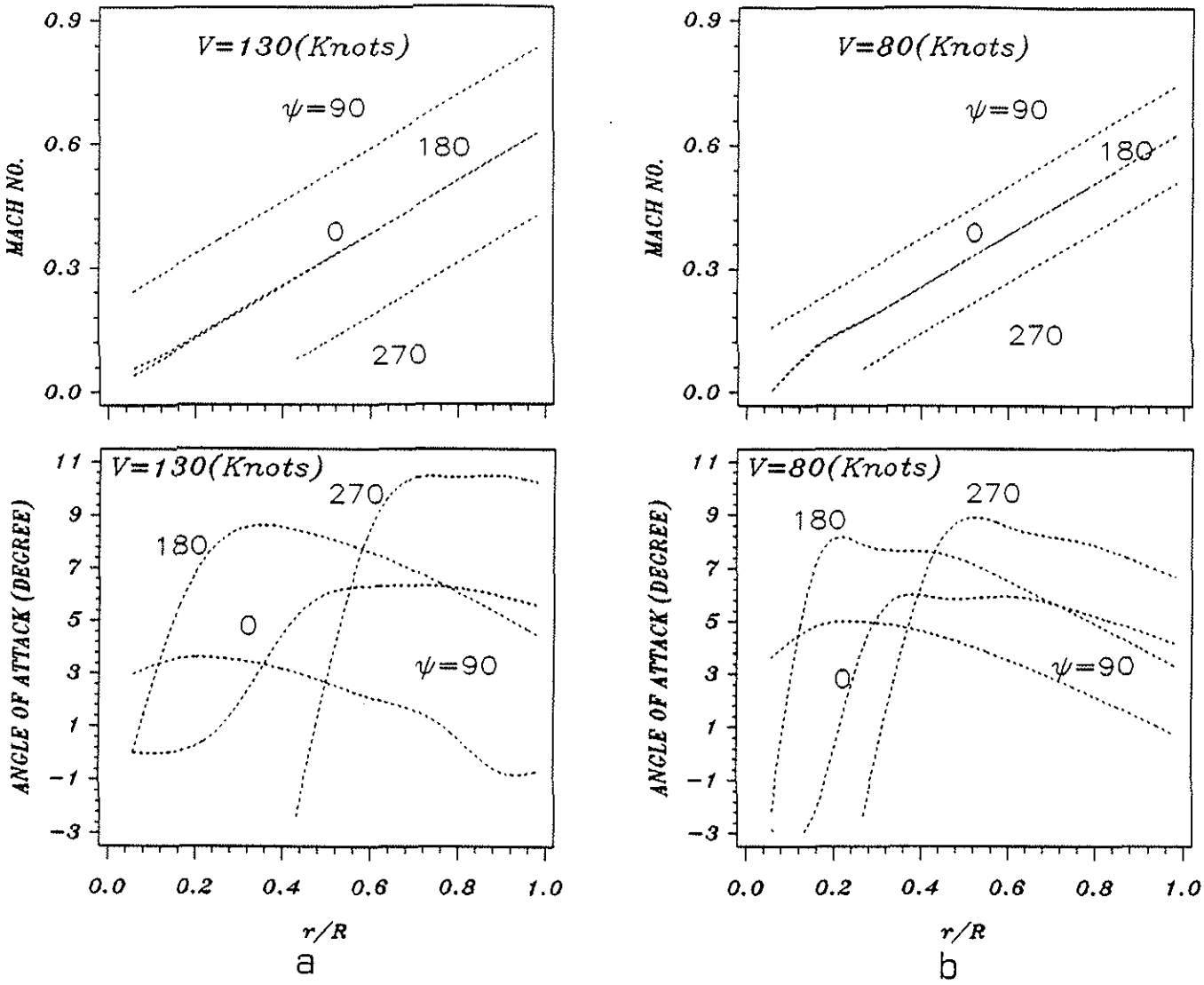

Fig. 3. Mach number and angle of attack spanwise distributions, at four azimuth angles (ψ=0°, 90°, 180°, 270°). a) 130 knots, b) 80 knots.

into Eqs. (24a-c) and numerical integrations result in the values of the harmonic coefficients. It is clear that by reducing the number of azimuthal locations where the loads are calculated, the required computations are significantly reduced. Therefore, the question of the minimal number of azimuthal points, which are necessary for convergence, is a crucial question concerning efficiency. In Fig. 5 the convergence of the blade resultant lift force, at an airspeed of 130 knots, while only one harmonic is used to describe the aerodynamic loads, is presented. Instead of indicating the number of azimuthal points, the azimuthal step (azimuthal distance between adjacent azimuthal points) is indicated. Azimuthal steps of 45°, 30°, 22.5° and 18° correspond to 8, 12, 16 and 20 azimuthal points, respectively. It can be concluded that the convergence with respect to the decreasing azimuthal step is very fast. An azimuthal step of 45° exhibits certain deviations, while an azimuthal step of 30° presents excellent convergence. The one-per-rev component exhibits excellent

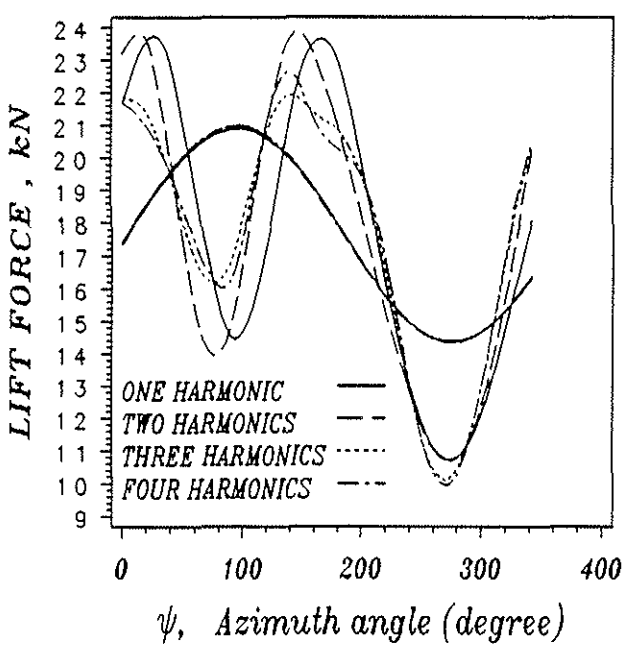

Fig. 4. The influence of the number of harmonics on the convergence of the resultant lift force of a blade at 130 knots.

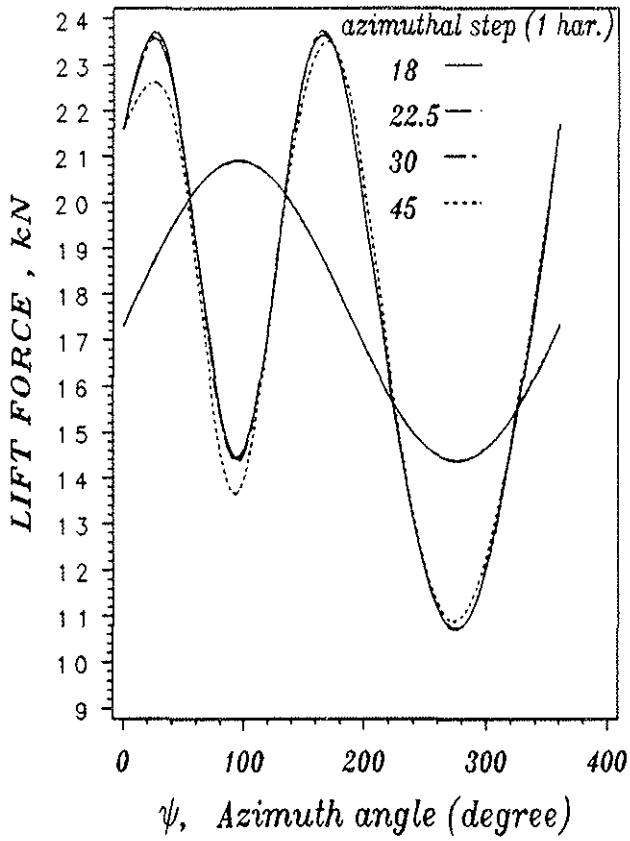

Fig. 5. The influence of the azimuthal step size on the convergence of the resultant lift force of a blade, at 130 knots. Only one harmonic is included in the calculations.

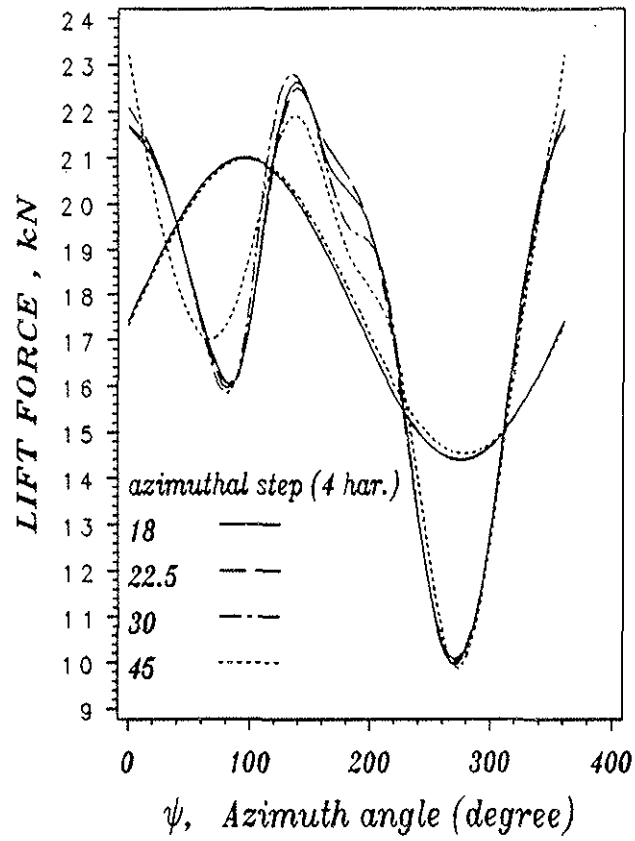

Fig. 6 The influence of the azimuthal step size on the convergence of the resultant lift force of a blade at 130 knots. Four harmonics are included in the calculations.

convergence for all the azimuthal steps.

When the number of harmonics is increased to four, the convergence with a decreasing azimuthal step is not as good as in the case of a single harmonic. This is clearly seen if Fig. 6 is compared with Fig. 5. In the case of azimuthal steps of 45°, significant deviations from the results for smaller azimuthal steps are clearly seen, whereas there are some deviations even in the one-per-rev component. Yet, a fairly fast convergence is obtained when the azimuthal step is further reduced. Very good convergence is obtained at azimuthal steps of 22.5° and 18°.

As indicated in subsection 3.2, in addition to the use of Eqs. (24a-c), the code offers the use of a FFT method to calculate the harmonic coefficients of the aerodynamic loads. Figure 7 presents a comparison between the lift force as obtained by using Eqs. (24a-c) with an azimuthal step of 18°, and a FFT technique with an azimuthal step of 4.4°. The agreement between the results is very good, presenting only negligible deviations. The one-per-rev components of both methods practically coincide.

In all the studies that were described above, the resultant blade lift was considered. Similar studies were also carried out considering other variables like the aerodynamic flapping moment or the blade resultant aerodynamic drag. The trends and behavior in all these cases were identical to those that were shown above. These results are not shown here because of lack of space.

5.2 Trim calculations

In Ref. 18 flight test results for a trimmed flight of an AH-64 are given. The helicopter weighs 65450 N (14940 lb), the longitudinal location of the center of mass is 5.134 m, while its lateral location is 0.02 m to the right. The flight tests were performed at an altitude of 1415 m and a temperature of 303°K.

The trim of the helicopter at the same conditions was calculated by the present mode and the results are shown in Figs. 8a-f. In all the figures the variables that define the trimmed flight are drawn as functions of the airspeed. The flight test results are compared with the calculations. In every figure five curves are shown. They represent calculations for values of N_j ranging between one harmonic and five harmonics.

It can be concluded that the convergence is very

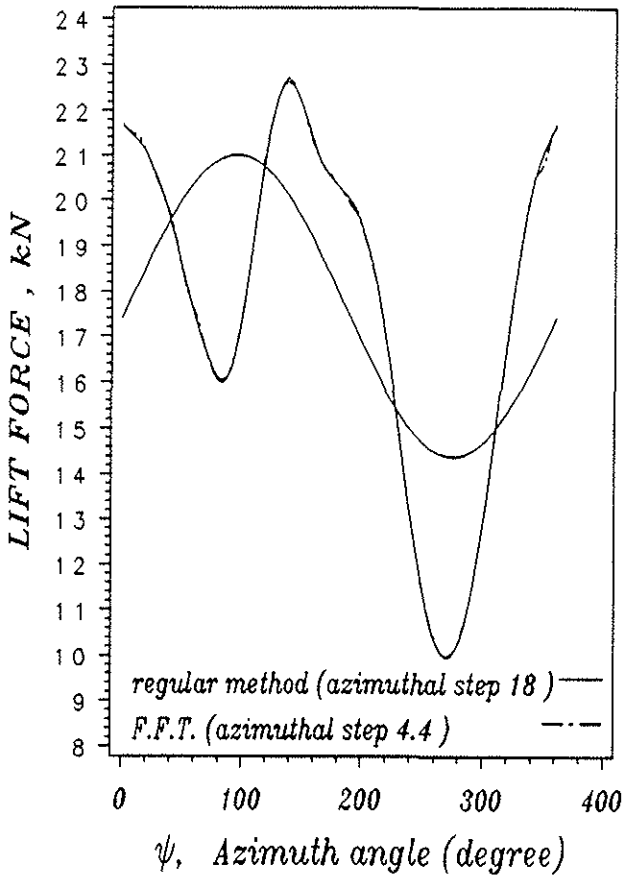

Fig. 7. Comparison between using Eqs. (24) and using a FFT method. The airspeed is 130 knots.

good throughout the entire range of airspeeds. At airspeeds below 75 knots the results for all the N_j values practically coincide. Above those airspeeds there are very small differences between the results, that grow as the airspeed increases. Careful examination of the results reveals that the largest differences usually appear between the results for one and two harmonics, and between two and three harmonics. The cases of three, four and five harmonics practically coincide. From a practical point of view, the differences between the majority of the calculations are negligible. The largest differences appear in the case of the fuselage pitch angle and the lateral control position, between the results for N_j=1,2 and the rest of the results (that exhibit very good convergence).

It is interesting to note that the directional control position (Fig. 8f) does not show any sensitivity to the number of harmonics.

The agreement between the flight test results and the calculations is quite good in the case of the collective and longitudinal control positions (Figs. 8a,b). The agreement in the case of the other variables is not as good, but still satisfactory. Since the agreement with flight test results is not the subject matter here, the subject will not be discussed any further. More comparisons between the results of the present model and flight test data are presented in Ref. 19.

5.3 Maneuvers

The subject of the influence of the rotor model on the simulation of helicopter maneuvers is very complicated and will probably appear in a future paper. Here only a brief discussion of a single aspect will be presented. The aspect that will be studied is the influence of the number of harmonics on the convergence of the helicopter response to a pilot command.

Studies, which are not presented here, have shown that in maneuvers starting from hover, where significant airspeeds are not developed, the influence of the number of harmonics is negligible. Thus, in order to obtain an efficient model it is recommended to us only a single harmonic in these cases.

In what follows a longitudinal maneuver, that starts from a trimmed flight at 80 knots, will be studied. The different pilot commands are presented in Fig. 9. The SCAS system is not operating. It is clearly shown that the longitudinal command is the dominant one.

The helicopter response is shown in Figs. 10a-d. Results for N_j values between one and five harmonics, are presented. In the case of the main axis (pitch) response (Fig. 10a) there is a very good convergence for N_j=4,5. N_j=3 exhibits some deviations beyond nine seconds. The case of N_j=1 shows the largest deviations from the converged results, while significant improvements are obtained for N_j=2. The C.G. normal acceleration (Fig. 10b) show similar trends, where the results for N_j=3-5 exhibit excellent convergence. In the case of the off-axis response (Figs. 10c,d) the convergence is again very good, and the cases of N_j=3,4,5 almost coincide. It should be noted that the deviations in the case N_j=2 are fairly small.

6. Conclusions

A new generic harmonic rotor model for helicopter flight simulation has been presented. This rotor model is based on a harmonic description of the aerodynamic loads, where only a finite number of harmonics are included in the complete calculations. The aerodynamic modeling is general and allows any level of sophistication. As the number of harmonics, which are included in the model, is increased, the accuracy is also increased. By including only a single harmonic, a model similar to a TPP model is obtained, where nonlinear aerodynamic effects are

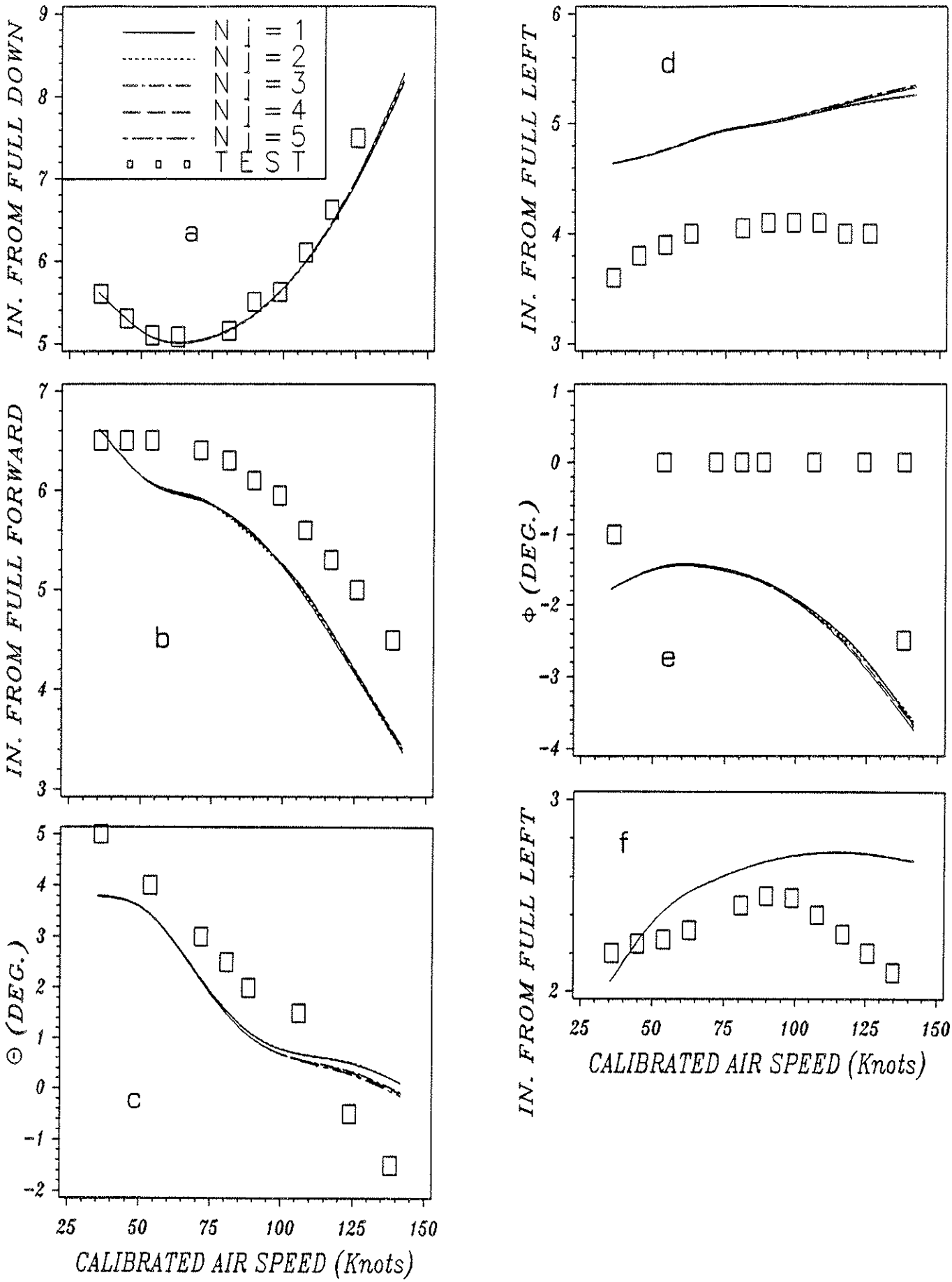

Fig. 8. The influence of the number of harmonics on the trim calculations. a) Collective control position. b) Longitudinal control position. c) Fuselage pitch angle. d) Lateral control position. e) Fuselage roll angle. f) Directional control position.

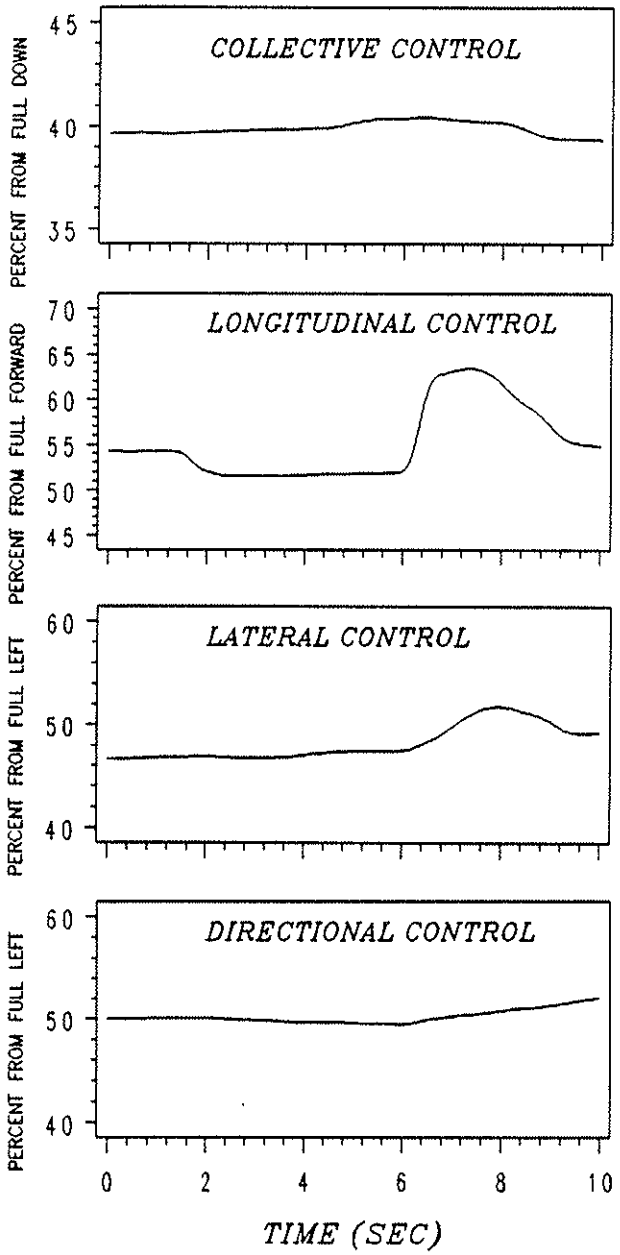

Fig. 9. Pilot commands during a longitudinal maneuver at 80 knots.

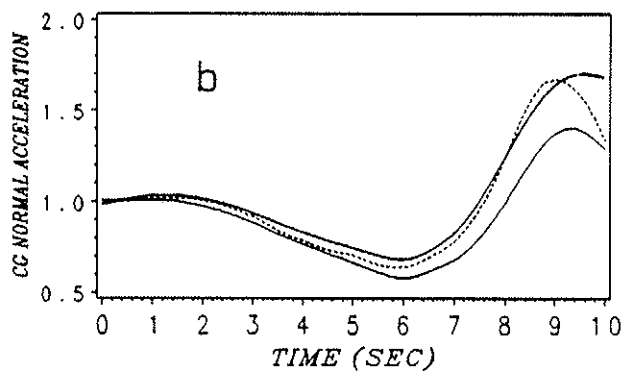

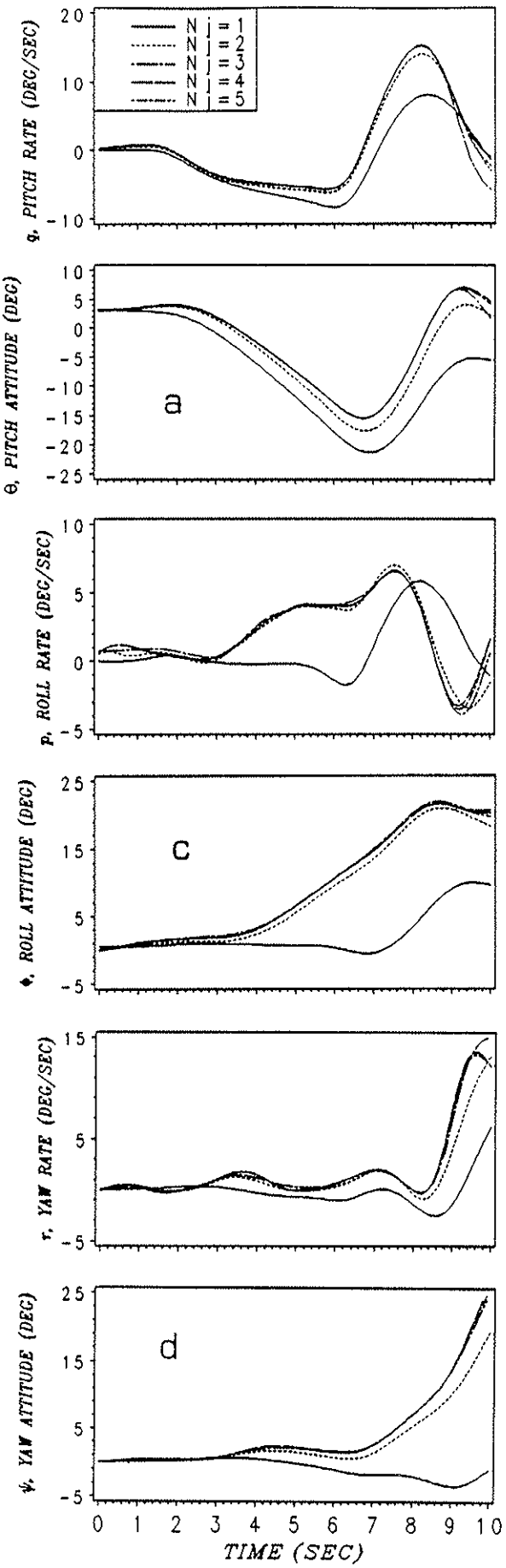

Fig. 10. The influence of the number of harmonics on the helicopter response. a) Pitch rate and pitch angle. b) C.G. normal acceleration. c) Roll rate and roll angle. d) Yaw rate and yaw angle.

also taken into account. If the number of harmonics is high, the model becomes equivalent to a direct blade-element approach.

As the number of harmonics (which are included in the model) is increased, the improved accuracy is accompanied by an increase in the required computing effort. The present model is unique in the sense that it offers a convenient way of obtaining a model that offers a certain balance between accuracy and efficiency. This balance can be very easily varied according to the nature of the problem.

Different studies have shown the very good convergence properties of the present model, with respect to the number of harmonics which are included, or the number of azimuthal points where the aerodynamic loads are calculated (and are used to further calculate the harmonic coefficients). As the number of azimuthal points is decreased, the model efficiency increases.

The studies included isolated rotor calculations, trim calculations and maneuvers. It has been shown that the convergence properties deteriorate as the airspeed is increased. Nevertheless, the present studies show that for trim calculations very good convergence is obtained by using only a single harmonic. In the case of maneuvers, increasing numbers of harmonics, depending on the airspeed, are required for good convergence. For maneuvers near hovering a single harmonic gives very good results.

Acknowledgment

The authors would like to thank Mr. H. Mansur and Dr. M. Tischler, of the U.S. Army AVSCOM, Aeroflight Dynamics Directorate, Ames Research Center, for their help with the flight test data and many fruitful discussions. They would also like to thank Mrs. A. Goodman for typing the manuscript.

References

1. Gessow, A., "Equations and procedures for numerically calculating the aerodynamic characteristics of lifting rotors", *NACA TN-3747*, October 1956.
2. Gessow, A. and Crim, A.D., "A theoretical estimate of the effects of compressibility on the performance of helicopter rotor in various flight conditions", *NACA TN-3798*, October 1956.
3. Bramwell, A.R.S., "*Helicopter Dynamics*", Eduards Arnolds Ltd., London, 1976.
4. Johnson, W., "*Helicopter Theory*", Princeton University Press, Princeton, N.J., 1980.
5. Stepniewski, W.Z. and Keys, C.N., "*Rotary-Wing Aerodynamics*", Dover Publications Inc., New York, 1984.
6. Howelett, J.J., "UH-60A Black Hawk engineering simulation program: Vol. 1 - Mathematical model", *NASA CR-166309*, December 1981.
7. Talbot, P.D., Tinling, B.E., Decker, W.A. and Chen, R.T.N., "A mathematical model of a single main rotor helicopter for piloted simulations", *NASA TM-84281*, 1982.
8. Beigelman, Z. and Rosen, A., "A simulation model of a single rotor helicopter", Proc. of the 31st Israel Annual Conf. on Aviation and Astronautics, February 21-22, 1990, pp. 27-37.
9. Harrison, J.M., "An integrated approach to effective analytical support helicopter design and development", 6th European Rotorcraft and Powered Lift Aircraft Forum, September 1980, Paper no. 40.
10. Rosen, A. and Beigelman, Z., "A simplified model of the influence of elastic pitch variations on rotor flapping dynamics", *Vertica*, Vol. 7, No. 4, 1983, pp. 335-360 (also Proc. of the 24th Israel Annual Conf. on Aviation and Aeronautics, 1982, pp. 225-237).
11. Rosen, A. and Beigelman, Z., "Further investigation of the coupled flapping and torsion dynamics of helicopter rotor blades", *Israel J. of Technology*, Vol. 21, 1983, pp. 104-116 (also Proc. of the 25th Israel Annual Conf. on Aviation and Aeronautics, February 1983, pp. 23-30).
12. Glauert, H., "A general theory of the autogyro", *ARC R&M 1111*, November 1926.
13. White, F. and Blake, B.B., "Improved method of predicting the helicopter control response and gust sensitivity", 35th AHS Annual Forum, May 1979, Paper No. 25.
14. Pitt, D.M. and Peters, D.A., "Theoretical prediction of dynamic inflow derivatives", *Vertica*, Vol. 5, No. 1, March 1981, pp. 21-34.
15. Bisplinghoff, R.L., Ashley, H. and Halfman, R.L., "*Aeroelasticity*", Addison-Wesley Publ. Co., 1957, p. 272.
16. Menaker, D. and Rosen, A., "A model for helicopter performances calculation", *Vertica*, Vol. 12, No. 1/2, 1988, pp. 155-178 (also Proc. of the 28th Israel Annual Conf. on Aviation and Astronautics, February 1986, pp. 111-129).
17. Rand, O., "Harmonic variable - a new approach to nonlinear periodic problems", *J. of Computers and Mathematics with Applications*, Vol. 15, No. 11, 1988, pp. 953-961.
18. U.S. Army, "Airworthiness and flight characteristics (A&FC) test of YAH-64 advanced attack helicopter", Final Report, USAAEFA Project No. 80-17-3, October 1982.
19. Mansur, M.H., Tischler, M.B, Chaimovitz, M., Rosen, A. and Rand, O., "Modeling methods for high-fidelity rotorcraft flight mechanics simulation", 16th European Rotorcraft Forum, 18-20 September, 1990, Paper No. III.II.2.1.
20. Chaimovitz, M., "Advanced Rotor Model for Flight Mechanics of Helicopter", M.Sc. Thesis (in Hebrew) Technion-I.I.T., July 1991.